

Electron Transfer in Nanoscale Contact Electrification: Effect of Temperature in the Metal–Dielectric Case

Shiquan Lin, Liang Xu, Cheng Xu, Xiangyu Chen, Aurelia C. Wang, Binbin Zhang, Pei Lin, Ya Yang, Huabo Zhao, and Zhong Lin Wang*

The phenomenon of contact electrification (CE) has been known for thousands of years, but the nature of the charge carriers and their transfer mechanisms are still under debate. Here, the CE and triboelectric charging process are studied for a metal–dielectric case at different thermal conditions by using atomic force microscopy and Kelvin probe force microscopy. The charge transfer process at the nanoscale is found to follow the modified thermionic-emission model. In particular, the focus here is on the effect of a temperature difference between two contacting materials on the CE. It is revealed that hotter solids tend to receive positive triboelectric charges, while cooler solids tend to be negatively charged, which suggests that the temperature-difference-induced charge transfer can be attributed to the thermionic-emission effect, in which the electrons are thermally excited and transfer from a hotter surface to a cooler one. Further, a thermionic-emission band-structure model is proposed to describe the electron transfer between two solids at different temperatures. The findings also suggest that CE can occur between two identical materials owing to the existence of a local temperature difference arising from the nanoscale rubbing of surfaces with different curvatures/roughness.

Contact electrification (CE) (or triboelectrification) was first noticed by ancient Greece about 2600 years ago, but its physics interpretation is not yet available and it is usually referred to as a negative effect. Fundamental study of this old and well-known phenomenon is a forgotten corner in basic physics. Nowadays, it rekindles the researchers' interest owing to the invention of triboelectric nanogenerators (TENGs), which uses triboelectric

charges for energy conversion.^[1–3] More triboelectric charges are required to be generated on insulator surfaces in TENG for higher output performance.^[4,5] However, the method to increase triboelectric charges in TENG is limited since the mechanism of CE still remains ambiguous. The biggest controversy in CE is the identity of the charge carriers and their transfer mechanism. It is well accepted that the charge transfer between two metals is due to electron transfer driven by the difference in the metal's work function.^[6] When the insulator is involved, the electron trapped in the surface states of insulator which can be excited into a conducting state is considered as the charge carriers.^[7–10] But some experiments also pointed out that the number of electrons in surface traps is insufficient to support the observed contact charging.^[11] And an opposing opinion is also widespread, which suggests that the CE involving insulator is caused by the transfer of mobile ions adsorbing on insulator surfaces^[12] or dissolving in the surface water layer.^[13,14]

ions adsorbing on insulator surfaces^[12] or dissolving in the surface water layer.^[13,14]

Very recently, Xu et al. have provided new evidences for the electron transfer in CE by performing the time-dependent experiments under different temperatures, and the dissipation of triboelectric charges was suggested to be caused by the thermionic emission of electrons for solid–solid cases.^[15] As inspired by the thermionic-emission model, we predict that the temperature may affect not only charge dissipation, but also charge transfer processes during CE, especially when the temperatures of two contact pairs are different. In fact, the temperatures of two solids which rub against each other are generally different due to the difference in material's thermal conductivity,^[16] surface roughness,^[17,18] asymmetric friction, etc. When two solids come into contact, electrons should be thermally excited more strongly at the hotter side, so they are more likely to transfer to the cooler side. Hence, the material at a higher temperature tends to be positively charged, while the material with a lower temperature tends to be negatively charged in CE. It is a very reliable method to determine the identity of the charge carriers by performing the CE between two solids at different temperatures. Also, if our prediction is verified, the temperature-difference-induced electron transfer could have general implication for studying CE between two identical materials with different

Dr. S. Lin, Prof. L. Xu, Prof. X. Chen, Dr. P. Lin, Prof. Y. Yang, Dr. H. Zhao, Prof. Z. L. Wang
Beijing Institute of Nanoenergy and Nanosystems
Chinese Academy of Sciences
Beijing 100083, P. R. China
E-mail: zlwang@binn.cas.cn

Dr. S. Lin, Prof. L. Xu, Prof. X. Chen, Dr. P. Lin, Prof. Y. Yang, Dr. H. Zhao, Prof. Z. L. Wang
School of Nanoscience and Technology
University of Chinese Academy of Sciences
Beijing 100049, P. R. China

Prof. C. Xu, Dr. A. C. Wang, Dr. B. Zhang, Prof. Z. L. Wang
School of Materials Science and Engineering
Georgia Institute of Technology
Atlanta, GA 30332-0245, USA

 The ORCID identification number(s) for the author(s) of this article can be found under <https://doi.org/10.1002/adma.201808197>.

DOI: 10.1002/adma.201808197

shapes/sizes, in which case the two sides could have different local temperatures owing to the geometrical effect on local heat dissipation process,^[19–21] which may result in electron transfer across interface.

In this study, the charge transfer between contacting metal and dielectric was investigated by using atomic force microscopy (AFM) and Kelvin probe force microscopy (KPFM).^[22–26] The effect of temperature on charge transport was studied, and the thermionic emission of electrons was first verified as the basic mechanism of CE at nanoscale for metal–dielectric case. Our conclusions were verified by controlling the temperature difference between the metal tip and the dielectric surface.

In our experiments, a Au-coated silicon tip was used as the metal contact side and the counterinsulator material sample was chosen as flat ceramics thin films, such as SiO₂, Si₃N₄, Al₂O₃, and AlN, deposited on high doped silicon wafers. The CE between the tip and the sample was performed under various temperatures, and the triboelectric charges on the insulator surface were measured in the KPFM mode. The entire AFM temperature control module apparatus was placed inside a closed chamber filled with Ar, as shown in Figure 1a. The tip temperature was controlled by the tip heater and insulator material was set at a temperature controlled by the sample heater. Hence, the temperatures of the tip and the sample could be controlled and monitored independently.

In previous studies, the triboelectric charges were usually generated by AFM in contact mode, in which the tip directly rubs

on the sample surface.^[27–29] In order to avoid friction heating, tip abrasion and heat exchange between the tip and sample introduced by rubbing, the peakforce tapping mode was used to generate triboelectric charges here. In the peakforce tapping mode, the tip contacts the sample surface point by point, and the force curve is shown in Figure 1b. The tip approaches the sample surface until the contact force reaches the set peakforce (≈ 10 nN in our experiments), and then the tip is withdrawn from the sample surface. In the experiments here, the time of the whole contact cycle for each point was about 1×10^{-3} s, hence the heat exchange between the tip and the sample was limited (the calculations are shown in the Supporting Information). Because there was no lateral friction in the peakforce tapping mode, both the friction heating and tip abrasion could be avoided. Figure 1c,d presents the tip topography before peakforce tapping, and Figure 1e,f gives the tip topography after peakforce tapping for more than 6.5×10^5 times. There was no visible tip damage observed in the scanning electron microscopy (SEM) images. Figure 1g shows the roughness of the SiO₂ sample surface, Figure 1h gives the array of X-ray photoelectron spectroscopy (XPS) detecting spots, and Figure 1i shows the XPS spectrum of the first detecting spot on the SiO₂ sample (XPS spectrums of other eight red spots are shown in Figure S1 in the Supporting Information). The roughness of the SiO₂ sample and the XPS spectrums show that the SiO₂ sample was uniform in composition and topography.

Here, the effect of temperature on both triboelectric charge generation and charge decay was investigated at nanoscale.

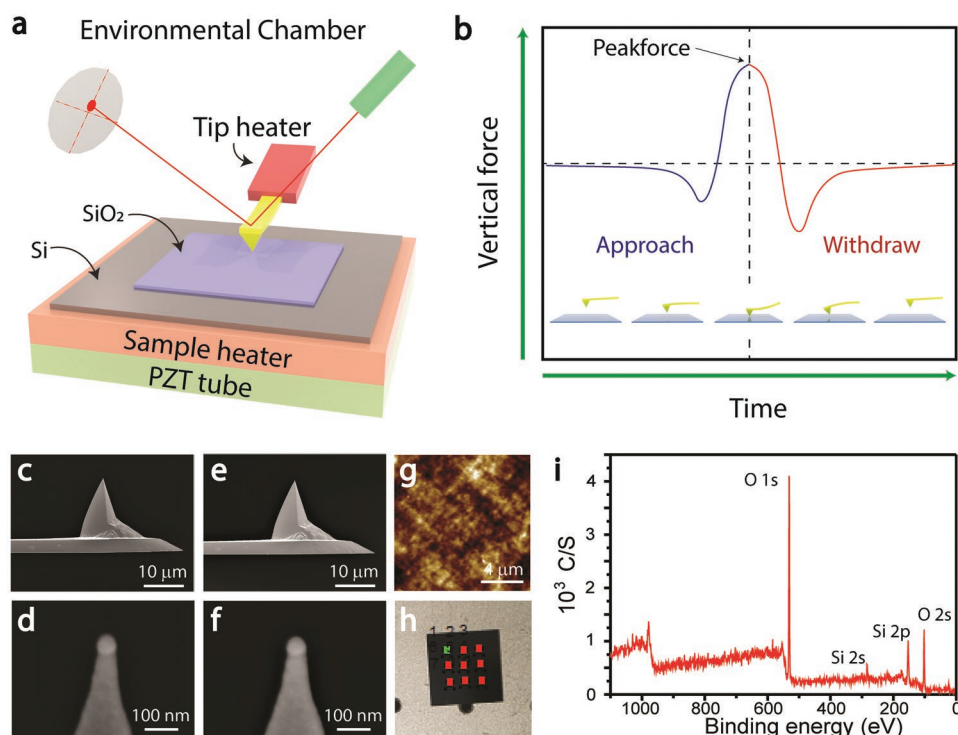


Figure 1. Schematic illustration of the AFM experiments. a) The setup of AFM experiment platform. b) The force curve of peakforce tapping mode. c,d) The SEM images of tip topography before peakforce tapping. e,f) The SEM images of tip topography after peakforce tapping for more than 6.5×10^5 times. g) The SiO₂ sample topography measured by AFM. h) The array of XPS detecting spots. i) The XPS spectrum of the SiO₂ sample.

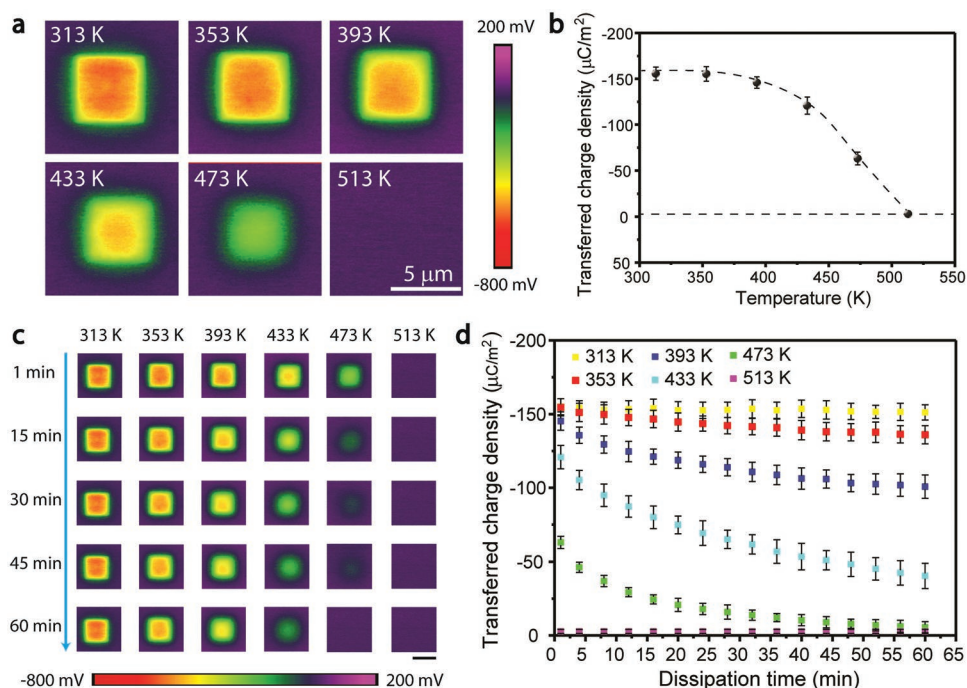


Figure 2. The triboelectric charge generation and dissipation on the SiO₂ sample surface at different temperatures. a) The change of SiO₂ sample surface potential induced by contacting with a Au-coated tip at different temperatures. b) The effect of temperature on the transferred charge density between the tip and the SiO₂ sample. c) The decay of the SiO₂ surface potential at different temperatures. d) The decay of transferred charge density on the SiO₂ surface at different temperatures.

The CE was performed at different temperatures (from 313 to 513 K), while the tip temperature maintained equal to the sample temperature. **Figure 2a** gives the change of SiO₂ sample surface potential induced by CE at various temperatures (the surface potential of the SiO₂ sample before contact charging is shown in Figure S2 in the Supporting Information). Based on the relationship between the surface potential and the charge density described in previous study,^[27] the transferred charge density on the sample surface was calculated and shown in Figure 2b. It was found that the SiO₂ sample was negatively charged when it was contacted by the Au-coated tip, and the magnitude of transferred charges decreased with increasing temperature. In particular, the triboelectric charge transfer was completely eliminated when the temperature increased to 513 K. This result agrees with the electron thermionic-emission theory in CE. At a low temperature (313 K), the electrons transferred from the tip to the SiO₂ sample when they are contacted with each other, and part of these electrons tunneled back when they were separated.^[30,31] And the observed triboelectric charges were the electrons left on the sample surface. When the temperature increased, more electrons tunneled back to the tip by thermionic emission. When the temperature increased to 513 K, all of the electrons tunneled back to the tip or escaped from the surface caused by thermal excitation, and there were no leftover transferred electrons. The results suggest that the thermionic emission can affect the triboelectric charge generation in CE at nanoscale.

After the CE, the charge dissipation experiment was performed at different temperatures for 60 min. Figure 2c gives the dissipation results of the surface potential, and the charge

density decay at different temperatures is shown in Figure 2d. The surface charges were found to decay faster at higher temperatures. According to the electron thermionic-emission model described in previous study,^[15] the surface charge follows an exponential decay as shown in the following equation

$$\sigma = e^{-at} \sigma_i \quad (1)$$

where σ denotes the surface charge density; a denotes the decay coefficient, which depends on the temperature, Richardson constant, Boltzmann constant, etc.; σ_i denotes the initial triboelectric charge density on the surface; and t is the dissipation time.

However, we found that Equation (1) did not fit our data well, as shown in Figure S3 (Supporting Information). In Figure 2d, part of the charges on the surface is difficult to be removed when the temperature is too low (313–433 K). Considering that some electrons may be tightly bounded by the surface states of the insulator material during CE, they may not contribute to the thermionic emission; we modified the electron thermionic-emission model as follows

$$\sigma = e^{-at} \sigma_e + \sigma_p \quad (2)$$

where σ_e denotes the triboelectric charges on the shallow surface and has contribution to the thermionic emission and σ_p denotes the triboelectric charges that remain on the surface “permanently.”

As shown in Figure S4 (Supporting Information), the modified thermal emission model fits our data perfectly. We noticed

that the ratio of σ_e to σ_p increased with rising temperature, which means that more electrons will be thermal excited so that they will transit out the bounding of the surface states. The results suggest that the charge decay also follows the thermal emission model at nanoscale.

Since the thermionic emission in CE was demonstrated, it is possible that the electrons would be thermally excited and transfer from the hotter material side to the cooler side. Hence, the charge transfer between the tip and the sample may be changed when the tip and the sample are set at different temperatures. To verify this, the tip and sample temperatures were controlled independently, and the tip temperature varied from 313 to 433 K, while the SiO_2 sample temperature varied from 403 K. The change of transferred charge density was found to be related to the temperature difference between the tip and the sample. As shown in **Figure 3**, the transferred charge density increased linearly with rising tip temperature, when the SiO_2 sample temperature maintained at 313, 343, 373, or 403 K, respectively. At a fixed tip temperature, the transferred charge density was found to decrease when the SiO_2 sample temperature was increased. These results are consistent with the thermionic-emission model. When the tip temperature increased, the electrons in the tip were excited and tended to hop from the tip to the SiO_2 sample, and the sample got more negatively charges. While the sample temperature increased, the electrons trapped on the SiO_2 surface states were excited and tended to hop from the sample to the tip, and the sample got fewer negative charges.

Further, the CE between the Au-coated tip and more materials, including Al_2O_3 , AlN and Si_3N_4 , was investigated, and the

results are shown in **Figure 4**. At 313 K, Al_2O_3 was negatively charged while Si_3N_4 was positively charged when they contacted with the Au-coated tip. It implies that Si_3N_4 is more inclined to donate the electron compared with Al_2O_3 , AlN , and SiO_2 . As demonstrated in **Figure 4a,c,e**, when the tip and sample temperatures were increased simultaneously, the magnitude of transferred charges on these sample surfaces decreased, which was the result of electron thermionic emission from the sample.

When the tip temperature was increased and the sample temperature maintained at 313 K, the transferred charges on the sample surfaces became more negative, as shown in **Figure 4b,d,f**. For the Al_2O_3 , the magnitude of the negative charges on the surface increased when the tip temperature was increased. The transferred charge density on the AlN surface was almost zero when the tip temperature equaled the sample temperature. However, the AlN got more negative charges when the tip temperature was higher than the sample temperature. Interestingly, different from the other three materials, the CE charges on Si_3N_4 were positive, and their density dropped with the increase of system temperature (**Figure 4e**). Furthermore, the charge density on Si_3N_4 experienced a sign reversal with the increase of tip temperature (**Figure 4f**). The results show that no matter the transferred charges are positive or negative when the tip temperature equals the sample temperature, more electrons are injected into the sample when the tip temperature increases. This is consistent with the thermionic-emission model, in which the electrons in the tip are excited when the tip temperature increases and are more likely to transfer to

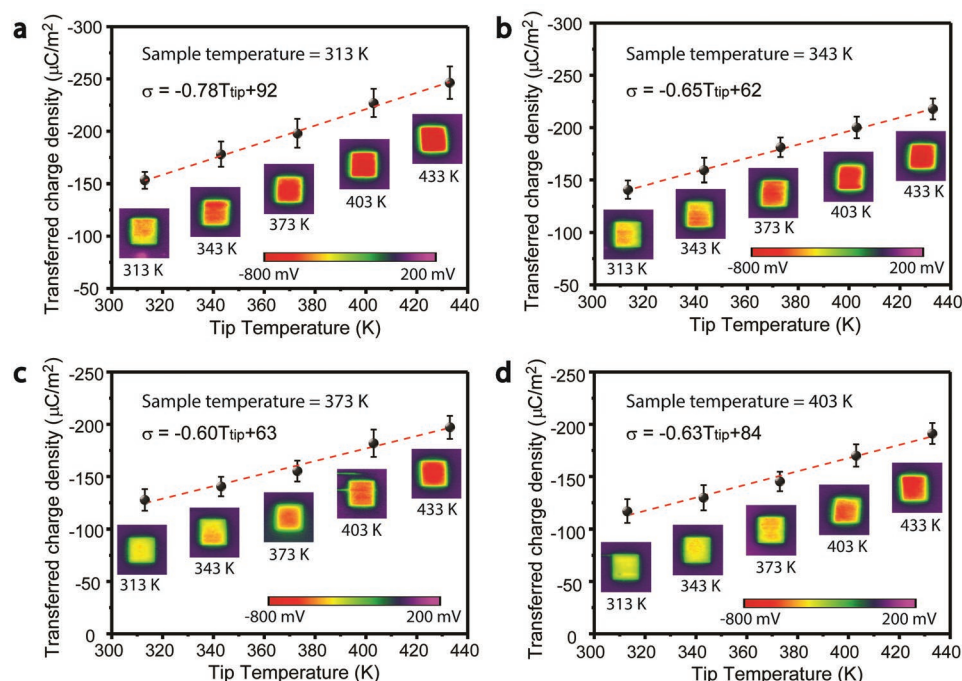


Figure 3. The effect of temperature difference on the CE between the Au-coated tip and the SiO_2 sample. The sample temperature was set at: a) 313 K, b) 343 K, c) 373 K, and d) 403 K, respectively, while the tip temperature varied from 313 to 433 K.

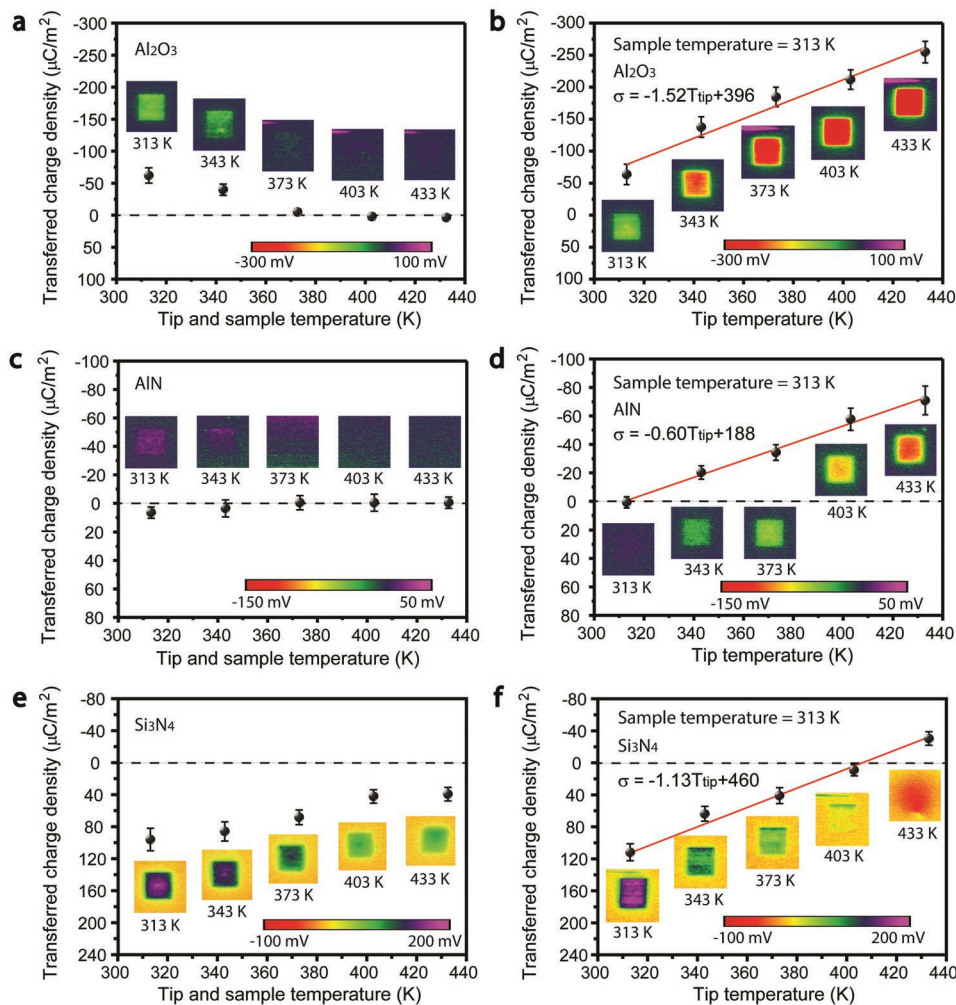


Figure 4. The effect of Au-coated tip and sample temperature difference on the CE between the tip and Al₂O₃, AlN, and Si₃N₄ flat samples. a,c,e) The change of transferred charge density on the Al₂O₃ (a), AlN (c), and Si₃N₄ (e) surfaces when both the tip and sample temperature increased. b,d,f) The relation between transferred charge density on the Al₂O₃ (b), AlN (d), and Si₃N₄ (f) surfaces and the tip temperature when the sample temperature is maintained at 313 K.

the sample, making the triboelectric charges on the sample surface more negative.

Here, a band-structure model is proposed to explain the temperature-difference-induced charge transfer between the metal and the dielectric. In the metal, the distribution of electrons at different energy follows the Fermi–Dirac function, as shown in the following equation

$$f(E) = \frac{1}{\text{EXP}((E - E_f)/kT) + 1} \quad (3)$$

where $f(E)$ denotes the probability of an electron in the energy level E , E_f denotes the Fermi level of the metal, k denotes the Boltzmann constant, and T is the temperature.

According to Equation (3), the electrons in the metal will be thermally excited and the increased electron energy is approximately kT . As shown in Figure 5a, we assume that the Fermi level (E_f) of the metal is higher than the highest occupied surface state level (E_0) of the dielectric, and the metal temperature

(T_m) lower than the dielectric temperatures (T_d) ($T_m < T_d$), hence the energy increase of electrons in the metal ($\sim kT_m$) will be lower than the increase of electron energy in the dielectric ($\sim kT_d$). In this case, the electrons transfer from the metal to the dielectric in the CE, as shown in Figure 5b. If the dielectric temperature is decreased, the metal temperature remains unchanged ($T_m = T_d$), as shown in Figure 5c. The energy increase of electrons in the metal ($\sim kT_m$) will be equal to the increase of electron energy in the dielectric ($\sim kT_d$), which leads to more electrons hopping from the metal to the dielectric than the situation when the metal temperature (T_m) is lower than the dielectric temperatures, as shown in Figure 5d. If the metal temperature is increased, the dielectric temperature remains unchanged ($T_m > T_d$), as shown in Figure 5e. The energy increase of electrons in the metal ($\sim kT_m$) will be higher than the increase of electron energy in the dielectric ($\sim kT_d$), which leads to more electrons hopping from the metal to the dielectric, as shown in Figure 5f. Since the dielectric temperature remains unchanged, the amount of electron tunneling back to the metal during the

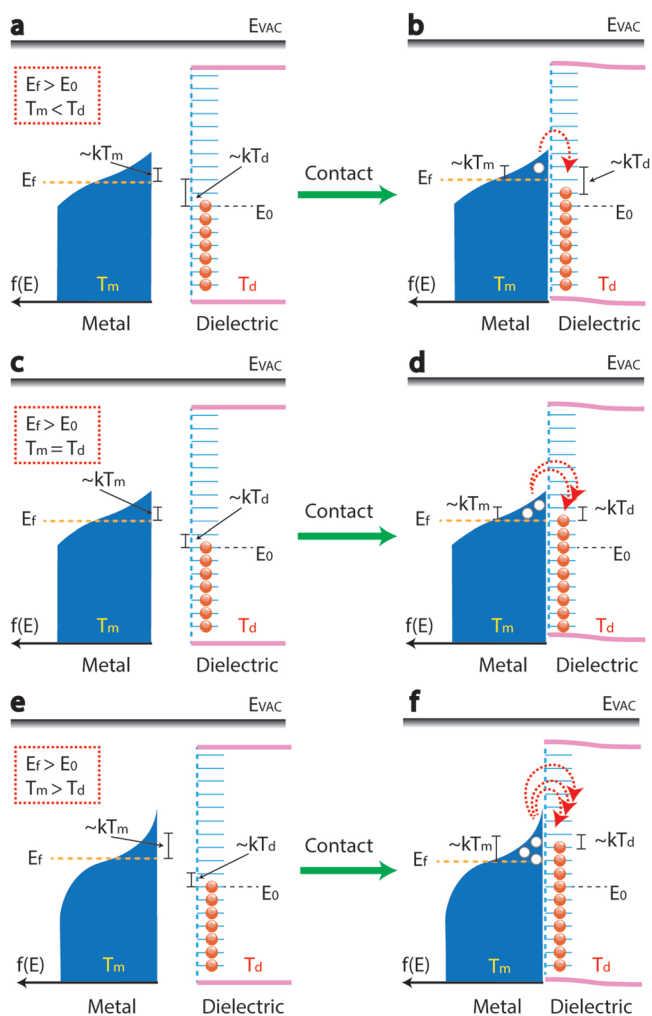


Figure 5. The band-structure model of the temperature-difference-induced charge transfer ($E_f > E_0$). a,c,e) The band structure of the metal and surface states of the dielectric, when the metal temperature is lower than the dielectric temperature (a), the metal temperature equals the dielectric temperature (c), and the metal temperature is higher than the dielectric temperature (e). b,d,f) Illustration of the contact charge transfer between the metal and the dielectric, when the metal temperature is lower than the dielectric temperature (b), the metal temperature equals the dielectric temperature (d), and the metal temperature is higher than the dielectric temperature (f).

separation almost remains unchanged. Hence, the triboelectric charges on the dielectric surface increase in this case.

In an alternative scenario, if the Fermi level of the metal is lower than the highest occupied surface state level of the dielectric, and the metal temperature equals the dielectric temperature, as shown in Figure 6a. The electrons will transfer from the dielectric to the metal, and the dielectric will be positively charged, as shown in Figure 6b. When the metal temperature is increased, and the dielectric temperature remains unchanged ($T_m > T_d$), as shown in Figure 6c. The energy increase of electrons in the metal will be higher than the increase of electron energy in the dielectric. The gap between the effective Fermi level of the metal and the highest occupied surface state level of the dielectric becomes smaller,

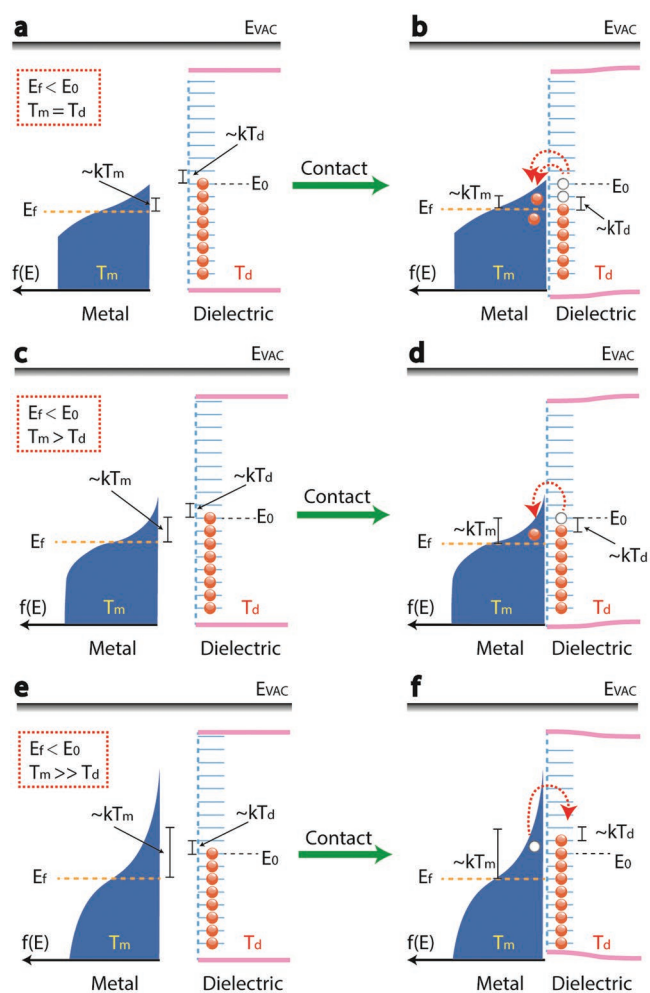


Figure 6. The band-structure model of the temperature-difference-induced charge transfer ($E_f < E_0$). a,c,e) The band structure of the metal and surface states of the dielectric, when the metal temperature equals the dielectric temperature (a), the metal temperature is higher than the dielectric temperature (c), and the metal temperature is much higher than the dielectric temperature (e). b,d,f) Illustration of the contact charge transfer between the metal and the dielectric, when the metal temperature equals the dielectric temperature (b), the metal temperature is higher than the dielectric temperature (d), and the metal temperature is much higher than the dielectric temperature (f).

which leads to less electron hopping from the dielectric to the metal, and the dielectric receive fewer positive charges in the CE, as shown in Figure 6d. In particular, if the metal temperature continues to increase and the dielectric temperature remains unchanged ($T_m \gg T_d$), the effective Fermi level of the metal will be higher than the highest occupied surface state level of the dielectric, as shown in Figure 6e. And the electrons will transfer from the metal to the dielectric, and the polarity of the transferred charge in the CE is reversed (Figure 6f), as we observed in the CE between the Au-coated tip and Si_3N_4 .

Further, the effect of temperature difference on the CE is analyzed quantitatively. According to the surface state model, the polarity and magnitude of transferred charges between the

metal and the dielectric depend on the metal's Fermi level (E_f), the highest occupied surface state level (E_0) of the dielectric and the surface state density of the dielectric ($N(E)$). When the temperature is 0 K, the transferred charge density on the dielectric surface in CE can be calculated as

$$\sigma = -e \int_{E_0}^{E_f} N(E) dE \quad (4)$$

where e denotes the elementary charge.

Based on our band-structure model, the electron's energy will increase when the temperature is increased, and Equation (4) can be expressed as follows

$$\sigma = -e \int_{E_0 + kT_d}^{E_f + kT_m} N(E) dE \quad (5)$$

where T_m denotes the metal temperature and T_d denotes the dielectric temperature.

When the dielectric temperature remains unchanged, the derivative of the transferred charge density to the metal temperature can be deduced as follows

$$\frac{d\sigma}{dT_m} = -ekN(E_f + kT_m) \quad (6)$$

where $N(E_f + kT_m)$ is a function that denotes the surface state density of the dielectric at the $E_f + kT_m$ energy level.

This means that the relation between transferred charge density and metal temperature is linear, which is consistent with the experimental results in Figures 3 and 4. Also, the slope between the transferred charges and metal temperature depends on the surface state density of the dielectric at the energy level $E_f + kT_m$. The relation between transferred charge density and tip temperature was linearly fitted in Figures 3 and 4, and the slope was calculated. According to Equation (6), the surface state density of SiO_2 , Si_3N_4 , Al_2O_3 , and AlN was calculated to be 4.71×10^{12} , 8.18×10^{12} , 11.01×10^{12} , and $4.34 \times 10^{12} \text{ eV}^{-1} \text{ cm}^{-2}$, respectively.

In order to further verify the thermionic-emission model in CE, experiments were performed under different DC biases applied between the tip and the dielectric. Figure 7a shows the effect of tip temperature on the transferred charge density between a Au-coated tip and SiO_2 sample, when different DC biases were applied and the sample temperature was set at 313 K. At any DC bias, the transferred charge density was found to be more negative when the tip temperature rose up. It suggests that the CE still follow the electron thermionic-emission model when the DC bias is applied at the interface. In particular, positive biases (3 and 4.5 V) between the tip and the SiO_2 sample lead to sign reversing of charge transfer in the experiments. This phenomenon can be explained by the proposed band-structure model. Without DC bias, the Fermi level of the Au-coated tip is higher than the highest occupied surface state level of the SiO_2 sample, and the electron transfer from the tip to the SiO_2 sample is shown in Figure 5a,b. When a negative bias is applied to the tip, the effective Fermi level of the tip goes up, and more electrons will transfer from the tip to the SiO_2 sample, as shown in Figure 7b. When the tip

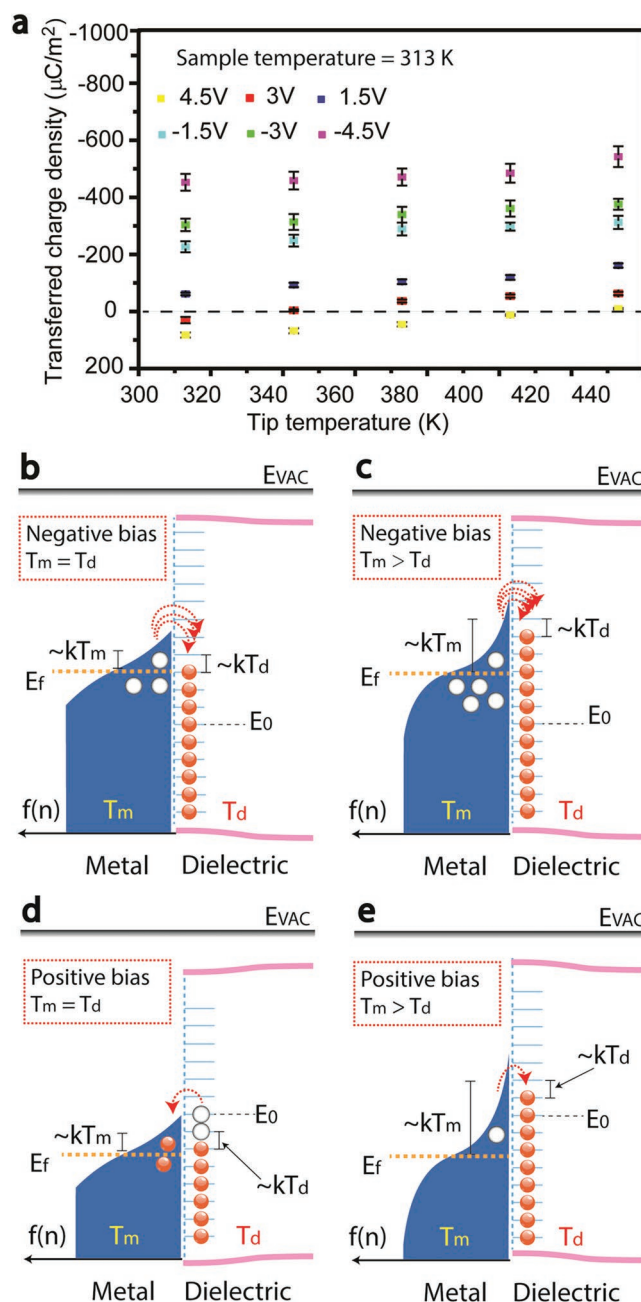


Figure 7. The robustness tests the thermionic-emission model in CE. a) The effect of tip temperature on the charge transfer between the Au-coated tip and the SiO_2 sample under various DC biases. b,c) The band structure of the metal and the dielectric when a negative bias is applied to the metal, while the metal temperature equals the dielectric temperature (b) and the metal temperature is higher than the dielectric temperature (c). d,e) The band structure of the metal and the dielectric when a positive bias is applied to the metal, while the metal temperature equals the dielectric temperature (d) and the metal temperature is higher than the dielectric temperature (e).

temperature increases and the sample temperature remains unchanged ($T_m > T_d$), the electrons in the tip are thermally excited and the magnitude of electrons transferred from the tip to the sample further increase, as shown in Figure 7c.

And the transfer charge density on the SiO₂ sample surface can be up to $-550 \mu\text{C m}^{-2}$ in this case (Figure 7a). When a positive bias is applied to the tip, the effective Fermi level of the tip goes down. If the positive bias is high enough, the effective Fermi level will be lower than the highest occupied surface state level of the SiO₂ sample and the electrons will transfer reversely from the SiO₂ sample to the tip, as shown in Figure 7d. When the tip temperature increases, and higher than the critical value (343 K in 3 V case and 403 K in 4.5 V case), the electrons are excited in the tip and the transfer direction reverses (transfer from the tip to the SiO₂ sample), as shown in Figure 7e.

The discoveries here should have significance in both science and technology. For the science, the researchers have been confused by some phenomena in CE for decades, including the CE between identical materials^[21] and the polarity reverse in the CE.^[22–24] The temperature-difference-induced electron transfer provides a new explanation for these phenomena. Once two identical materials of different shapes/sizes rub against each other (such as a stick against a slab), the one with a sharp tip shape tends to have a high temperature than its counterpart because the limited thermal conductance, which may lead to the hopping of electrons from the sharper one to the flat one. Therefore, a temperature difference can affect not only the magnitude but also the polarity of transferred charges. In practice, since there is no perfect flat surface, when two surfaces are in contact, the local non-uniformity will result in a non-uniform contact, probably resulting in a small variation in local temperature across the surface, which is possible to influence the polarity of transferred charges.

In conclusion, we investigated the effect of temperature on metal–dielectric CE at nanoscale by using AFM and KPFM. The triboelectric charge decay was found to follow the thermionic-emission model at nanoscale. And the results suggest that the temperature difference can affect both the magnitude and polarity of transferred charges in CE. The hotter materials tend to be positively charged while the cooler materials tend to be negatively charged. Further, an electron transfer mechanism based on thermionic-emission model was proposed to explain the effect of temperature on metadielectric CE. Moreover, the findings here give a possible explanation for the CE between identical materials, polarity reverse in CE and provide a potential method to control the CE in TENG by changing the temperature difference.

Experimental Section

Sample Preparation: The SiO₂, Si₃N₄, Al₂O₃, and AlN layer of 100 nm in thickness were deposited on high doped silicon surfaces by thermal oxidation, plasma-enhanced chemical vapor deposition, atomic layer deposition and magnetron sputtering, respectively.

Temperature Control: The sample was heated by the sample heater and its temperature was monitored by a temperature sensor under the sample. The volume of the tip heater was much larger than the tip volume, hence the tip temperature was approximately equal to the tip heater temperature when they reached thermal equilibrium. The tip cantilever would deflect when the tip temperature was changed, and the cantilever deflection was monitored to determine whether the tip and the tip heater were in thermal equilibrium.

AFM Experiments: The experiments were performed on a commercial AFM/KPFM equipment Multimode 8 (Bruker, USA). The conductive tip used here is NSC 18 (MikroMash, USA; coating: Au; tip radius: 25 nm; spring constant: 2.8 N m⁻¹). Before the experiments, the tip and the sample were both heated to 473 K and maintained for 30 min in Ar atmosphere first, to remove the water molecules on the sample surface. Then, the CE was performed in peakforce tapping mode under different temperatures. In the peakforce tapping scanning, the scan size was set to 5 μm , scan rate was 4 Hz and peakforce was ≈ 10 nN. Then, the triboelectric charges were detected in KPFM mode immediately, while the tapping amplitude was set to 350 mV, the lift height was 50 nm and the scan size was 10 μm .

Supporting Information

Supporting Information is available from the Wiley Online Library or from the author.

Acknowledgements

Research was supported by the National Key R&D Project from Minister of Science and Technology (2016YFA0202704), Beijing Municipal Science & Technology Commission (Z171100000317001, Z171100002017017, and Y3993113DF), and National Natural Science Foundation of China (Grant Nos. 51432005, 5151101243, 51561145021, and 51605033).

Conflict of Interest

The authors declare no conflict of interest.

Keywords

contact electrification, electron transfer, Kelvin probe force microscopy, temperature effect

Received: December 20, 2018

Revised: January 29, 2019

Published online:

- [1] F. Fan, Z. Tian, Z. L. Wang, *Nano Energy* **2012**, *1*, 328.
- [2] G. Zhu, B. Peng, J. Chen, Q. Jing, Z. L. Wang, *Nano Energy* **2015**, *14*, 126.
- [3] Z. L. Wang, *ACS Nano* **2013**, *7*, 9533.
- [4] Y. Mao, D. Geng, E. Liang, X. D. Wang, *Nano Energy* **2015**, *15*, 227.
- [5] J. Lee, H. Cho, J. Chun, K. Kim, S. Kim, C. Ahn, I. Kim, J. Kim, S. Kim, C. Yang, J. Baik, *Sci. Adv.* **2017**, *3*, e1602902.
- [6] J. Lowell, *J. Phys. D: Appl. Phys.* **1975**, *8*, 53.
- [7] K. Byun, Y. Cho, M. Seo, S. Kim, S. Kim, H. Shin, S. Park, S. Hwang, *ACS Appl. Mater. Interfaces* **2016**, *8*, 18519.
- [8] J. Wu, X. Wang, H. Li, F. Wang, W. Yang, Y. Hu, *Nano Energy* **2018**, *48*, 607.
- [9] J. Lowell, *J. Phys. D: Appl. Phys.* **1977**, *10*, 65.
- [10] J. C. Angus, I. Greber, *J. Appl. Phys.* **2018**, *123*, 174102.
- [11] R. Waitukaitis, V. Lee, J. M. Pierson, S. L. Forman, H. M. Jaeger, *Phys. Rev. Lett.* **2014**, *112*, 218001.
- [12] L. S. McCarty, G. M. Whitesides, *Angew. Chem., Int. Ed.* **2008**, *47*, 2188.
- [13] J. Wiles, M. Fialkowski, M. Radowski, G. M. Whitesides, *J. Phys. Chem. B* **2004**, *108*, 20296.

- [14] S. Pence, V. Novotny, A. Diaz, *Langmuir* **1994**, *10*, 592.
- [15] C. Xu, Y. Zi, A. C. Wang, H. Zai, Y. Dai, X. He, P. Wang, Y. Wang, P. Feng, D. Li, Z. L. Wang, *Adv. Mater.* **2018**, *30*, 1706790.
- [16] H. A. Abdel-Aal, *Int. Commun. Heat Mass Transfer* **1997**, *24*, 241.
- [17] F. Shen, K. Zhou, *Int. J. Mech. Sci.* **2018**, *148*, 94.
- [18] W. Qin, X. Jin, A. Kirk, P. H. Shipway, W. Sun, *Tribol. Int.* **2018**, *120*, 350.
- [19] D. Kim, J. H. Lee, I. You, J. K. Kim, U. Jeong, *Nano Energy* **2018**, *50*, 192.
- [20] X. Y. Yan, G. Zhu, Z. L. Wang, *Nano Energy* **2014**, *10*, 83.
- [21] R. Rham, R. C. Virnelson, R. M. Sankaran, D. J. Lacks, *J. Electrostat.* **2011**, *69*, 456.
- [22] B. D. Terris, J. E. Stern, D. Rugar, H. J. Mamin, *Phys. Rev. Lett.* **1989**, *63*, 2669.
- [23] H. T. Baytekin, A. Z. Patashinski, M. Branicki, S. Soh, B. A. Grzybowski, *Science* **2011**, *333*, 308.
- [24] S. Lin, T. Shao, *Phys. Chem. Chem. Phys.* **2017**, *19*, 29418.
- [25] M. Nonnenmacher, M. P. O'Boyle, H. K. Wickramasinghe, *Appl. Phys. Lett.* **1991**, *58*, 2921.
- [26] C. Schonenberger, S. F. Alvarado, *Phys. Rev. Lett.* **1990**, *65*, 3162.
- [27] Y. S. Zhou, Y. Liu, G. Zhu, Z. H. Lin, C. Pan, Q. Jing, Z. L. Wang, *Nano Lett.* **2013**, *13*, 2771.
- [28] Y. S. Zhou, S. Wang, Y. Yang, G. Zhu, S. Niu, Z. Lin, Y. Liu, Z. L. Wang, *Nano Lett.* **2014**, *14*, 1567.
- [29] H. Sun, H. Chu, J. Wang, L. Ding, Y. Li, *Appl. Phys. Lett.* **2010**, *96*, 083112.
- [30] G. S. Rose, S. G. Ward, *Br. J. Appl. Phys.* **1957**, *8*, 121.
- [31] J. Lowell, *J. Phys. D: Appl. Phys.* **1979**, *12*, 1541.